

Case Report

## Membranous Glomerulonephropathy in a Hatano Low-avoidance Rat

Kyohei Yasuno<sup>1</sup>, Haruka Sakashita<sup>1</sup>, Ryosuke Kobayashi<sup>1</sup>, Saori Araki<sup>1</sup>, Rio Saito<sup>1</sup>,  
Mariko Shiota<sup>2\*</sup>, Junichi Kamiie<sup>3</sup>, and Kinji Shitora<sup>1,3</sup>

<sup>1</sup> Research Institute of Biosciences, Azabu University, 1-17-71 Fuchinobe, Chuo-ku, Sagamihara, Kanagawa 252-5201, Japan

<sup>2</sup> Laboratory of Comparative Toxicology, School of Veterinary Medicine, Azabu University, 1-17-71 Fuchinobe, Chuo-ku, Sagamihara, Kanagawa 252-5201, Japan

<sup>3</sup> Laboratory of Veterinary Pathology, School of Veterinary Medicine, Azabu University, 1-17-71 Fuchinobe, Chuo-ku, Sagamihara, Kanagawa 252-5201, Japan

**Abstract:** Membranous glomerulonephropathy can be experimentally induced in rats, but spontaneous cases have been rarely reported. In this report, we present a typical case of spontaneous membranous glomerulonephropathy in a rat. A male Hatano low-avoidance (LAA) strain rat had a tumor mass on the right auricle, and was sacrificed at 41 weeks of age. Urinary screening by reagent strips revealed intense proteinuria. Histological tests revealed frequent presence of irregularly sized eosinophilic hyaline materials on the capillary wall and in the mesangium of renal glomeruli. Immunofluorescence revealed granular deposits of IgG, IgM, and C3 in the glomeruli. Subepithelial dense deposits were observed by electron microscopy accompanied by podocyte foot process effacement and occasional irregular thickening of the glomerular basement membrane. The rat also developed chronic lymphocytic pancreatitis, and the tumor mass on the right auricle was diagnosed as a fibrosarcoma. Screening tests for antibodies against major infectious agents and antinuclear antibody were negative. Western blot and indirect immunofluorescence analyses suggested the presence of an autoantibody against the pancreatic component. The glomerulopathy was considered an early stage of membranous glomerulonephropathy. (DOI: 10.1293/tox.26.203; J Toxicol Pathol 2013; 26: 203–208)

**Key words:** immunopathology, kidney, membranous glomerulonephropathy, nephrology, rat

Immune-mediated glomerulonephritis is a wide-spectrum disease, and representative examples are membranous nephropathy (MN), postinfectious glomerulonephritis, immunoglobulin A (IgA) nephropathy, lupus nephritis, anti-neutrophil cytoplasmic antibody (ANCA)-mediated disease, and anti-glomerular basement membrane (anti-GBM) glomerulonephritis. Even minimal change disease (MCD) and focal segmental glomerulosclerosis (FSGS) are included in this spectrum<sup>1</sup>. MN is a pathological condition characterized by a spectrum of changes in the GBM and is one of the most common forms of immune-mediated glomerulonephritis in adult humans. This condition can be idiopathic or secondary to various clinical conditions, including infections, systemic lupus erythematosus, cancer and drug intoxication<sup>2</sup>. In rats, Heymann nephritis could be used as a model of MN<sup>3</sup>, but spontaneous cases are rarely reported. In this report, we describe a typical case of spontaneous immune-mediated glomerulonephritis in a Hatano low-avoidance (LAA) rat.

A 41-week-old male LAA rat, an inbred strain genetically selected and bred from Sprague–Dawley (SD) rats<sup>4</sup>, had a dome-shaped, hard cutaneous mass (7 mm × 7 mm in diameter) on the right auricle. The rat was established from cryopreserved embryos of the LAA strain, which were supplied by the National BioResource Project for the Rat in Japan, Kyoto University (Kyoto, Japan). Alopecia and mild ulceration were observed on its surface. Urinary screening by reagent strips revealed prominent proteinuria (500 mg/dl), but no abnormalities were detected when it was tested for glucose, ketone bodies, bilirubin, urobilinogen, and occult blood. Serum antibody tests performed at the International Council for Laboratory Animal Science Monitoring Center, Central Institute of Experimental Animals, Kanagawa, Japan, revealed no infections of *Clostridium piliforme*, hantavirus, *Mycoplasma pulmonis*, Sendai virus, sialodacryoadenitis virus, cilia-associated respiratory bacillus, H-1 virus, Kilham rat virus, mouse minute virus, mouse adenovirus, mouse encephalomyelitis virus, mouse pneumonia virus, retrovirus type 3, *Corynebacterium kutscheri* or *Salmonella typhimurium*. Serum glucose (199 mg/dl), triglyceride (157 mg/dl) and total cholesterol (129 mg/dl) levels were nearly normal.

The rat was euthanized in accordance with the guidelines approved by the Animal Research Committee of Azabu University. At necropsy, no significant gross lesions were

Received: 15 January 2013, Accepted: 19 February 2013

\*Corresponding author: M Shiota (e-mail: m-shiota@azabu-u.ac.jp)

©2013 The Japanese Society of Toxicologic Pathology

This is an open-access article distributed under the terms of the Creative Commons Attribution Non-Commercial No Derivatives (by-nc-nd) License <<http://creativecommons.org/licenses/by-nc-nd/3.0/>>.

**Table 1.** Antibodies and Immunostaining Protocol

Primary antibody <sup>a</sup>	Clone	Dilution	Antigen retrieval <sup>b</sup>	Antibody source <sup>c</sup>
<b>Immunofluorescence</b>				
FITC-conjugated anti-rat IgG	Polyclonal	1:500	Trypsin	Cappel
FITC-conjugated anti-rat IgM	Polyclonal	1:500	Trypsin	Cappel
FITC-conjugated anti-rat IgA	Polyclonal	1:500	Trypsin	Nordic Immunological Lab.
FITC-conjugated anti-rat C3	Polyclonal	1:1000	Trypsin	Cappel
<b>Immunohistochemistry</b>				
Anti-rat CD3	G4.18	1:50	MW	BD Biosciences
Anti-CD20	Polyclonal	1:150	NT	Thermo Fisher Scientific
Anti-rat CD68	ED1	1:100	Trypsin	Serotec
Anti-glucagon	Polyclonal	Ready to use	Pepsin	Dako A/S
Anti-insulin	Polyclonal	Ready to use	NT	Dako A/S

<sup>a</sup> FITC = fluorescein isothiocyanate; Ig = immunoglobulin. <sup>b</sup> Trypsin = 0.1% trypsin (Dako A/S, Glostrup, Denmark), 37°C, 30 min; MW = microwave/citrate buffer pH 6.0, 90°C, 20 min; NT = no treatment; Pepsin = 0.4% pepsin (Sigma-Aldrich Co., St. Louis, MO, USA), 37°C, 20 min. <sup>c</sup> Cappel, Aurora, OH, USA; Nordic Immunological Laboratories, Eindhoven, The Netherlands; BD Biosciences, Franklin Lakes, NJ, USA; Thermo Fisher Scientific Inc., Waltham, MA, USA; Serotec, Wiesbaden, Germany.

found in the kidneys except for several small scars in the left kidney. The cut surface of the ear mass was white-to-gray and well demarcated with partial hemorrhage. Other organs were grossly normal, and pleural or peritoneal effusion was not detected.

Systemic organs, including the ear mass, were fixed in 10% neutral-buffered formalin, embedded in paraffin, sectioned and stained with hematoxylin and eosin (HE), periodic acid-Schiff (PAS), periodic acid methenamine silver (PAM), or Masson's trichrome stain.

For immunofluorescence analyses of the kidney, after incubation with 4% Block Ace<sup>TM</sup> (Snow Brand Milk Products Co., Ltd., Sapporo, Japan) for 10 min at room temperature, the dewaxed sections were incubated for 1 h at 37°C with the primary antibodies summarized in Table 1 and examined under an FSX100 fluorescence microscope (Olympus, Tokyo, Japan). Immunohistochemical staining was performed using the immunoenzyme polymer method with the primary antibodies summarized in Table 1. Peroxidase-conjugated anti-mouse IgG (Histofine Simple Stain MAX-PO (M); Nichirei, Tokyo, Japan) or anti-rabbit IgG (Histofine Simple Stain MAX-PO (R); Nichirei) was used as the secondary antibody. After immunoreaction, the sections were stained with diaminobenzidine and counterstained with Mayer's hematoxylin. Sections were also stained under identical conditions with normal mouse IgG or normal rabbit IgG to serve as negative controls.

Portions of the formalin-fixed tissue specimens from the kidney sample were cut into cubes of 1 mm<sup>3</sup>, refixed in 2.5% glutaraldehyde and postfixed in 1% OsO<sub>4</sub> for 2 h. These specimens were then dehydrated through ascending grades of alcohol and embedded in epoxy resin. Ultrathin sections were double-stained with uranyl acetate and lead citrate and examined using a JEM 1400 transmission electron microscope (JEOL Ltd., Tokyo, Japan) at 80 kV.

Western blotting was used to detect autoantibodies in the serum. Fresh liver or pancreas tissue from a 9-week-old

male normal SD rat was homogenized in a Dounce homogenizer in 1% sodium dodecyl sulfate (SDS). Eluted protein samples were run on a 10% SDS-polyacrylamide gel electrophoresis (SDS-PAGE) and subsequently transferred onto polyvinylidene fluoride membranes (Bio-Rad, Hercules, CA, USA). The membranes were blocked with 5% skim milk in PBS with 0.1% Tween 20 for 1 h at room temperature and incubated overnight with the serum from the present case or a normal SD rat at a concentration of 10 mg protein/ml at 4°C. After washing, the membranes were incubated with horseradish peroxidase (HRP)-conjugated polyclonal rabbit anti-rat Igs (Dako A/S, Glostrup, Denmark). Immunoreactivity was visualized using Luminata<sup>TM</sup> Forte Western HRP Substrate (Millipore, Temecula, CA, USA). In addition, indirect immunofluorescence tests targeting normal rat liver or pancreas tissues were performed using the serum from this rat. In particular, liver tissue was used to detect antinuclear antibodies. Unfixed cryostat sections (3 µm) of liver and pancreas of the 9-week-old male SD rat were washed with cold PBS. After incubation with 4% Block Ace<sup>TM</sup> (Snow Brand Milk Products Co., Ltd.) for 10 min at room temperature, the sections were incubated with 1 mg protein/ml serum of the present case or normal SD rat at 4°C overnight. After washing with cold PBS, the sections were incubated with fluorescein isothiocyanate (FITC)-conjugated rabbit anti-rat IgG (1:500; Cappel, Aurora, OH, USA) at room temperature for 30 min. Sections were observed under an FSX100 fluorescence microscope (Olympus).

Histological evaluation revealed that irregularly sized discrete eosinophilic hyaline materials were frequently present on the capillary walls and in the mesangium of the glomeruli in both kidneys of the LAA rat (Fig. 1). These materials were stained red by Masson's trichrome stain (Fig. 2). Several glomeruli included swollen podocytes with PAS-positive intracellular droplets and/or vacuoles (Fig. 3a), a thick GBM and increased mesangial matrix. Adhesions between the capillary tufts and Bowman's capsules (Fig. 3b)

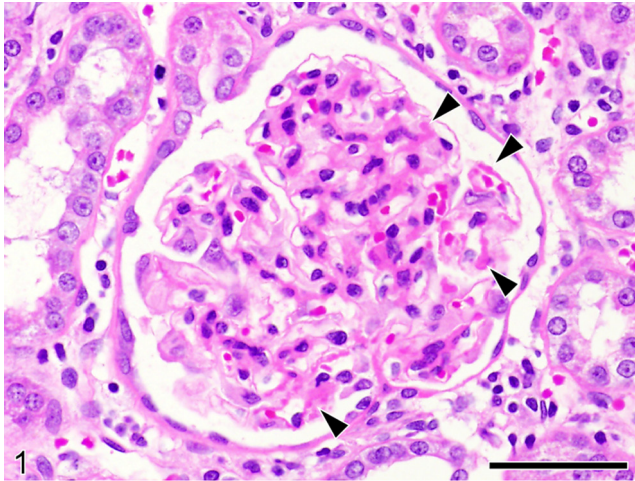


**Fig. 1.** Glomerulus of a 41-week-old, male Hatano low-avoidance (LAA) rat. Irregular discrete eosinophilic materials are present on the capillary wall and in the mesangium (arrowheads). Hematoxylin and eosin (HE) stain. Bar = 50  $\mu$ m.

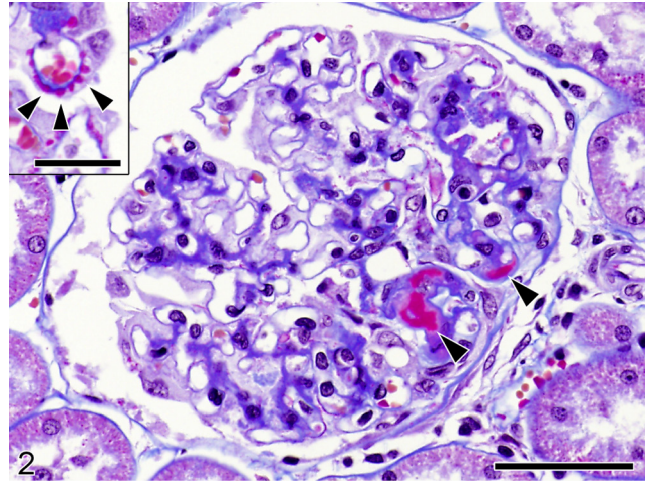


**Fig. 2.** Masson's trichrome staining of Hatano low-avoidance (LAA) rat glomerulus. Red-colored deposits are present at the mesangium and on the capillary wall (arrowheads). Bar = 50  $\mu$ m. Small deposits (arrowheads) are present discretely along the capillary wall (inset, Bar = 20  $\mu$ m).

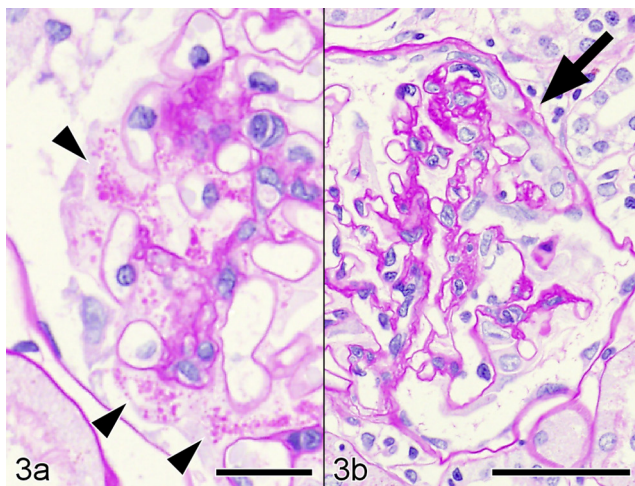


**Fig. 3.** Glomeruli of the Hatano low-avoidance (LAA) rat. (a) Many fine hyaline droplets are present in the swollen podocyte (arrowheads). Stained with periodic acid-Schiff. Bar = 30  $\mu$ m. (b) Adhesion between the tuft and Bowman's capsule (arrow). Bar = 50  $\mu$ m.

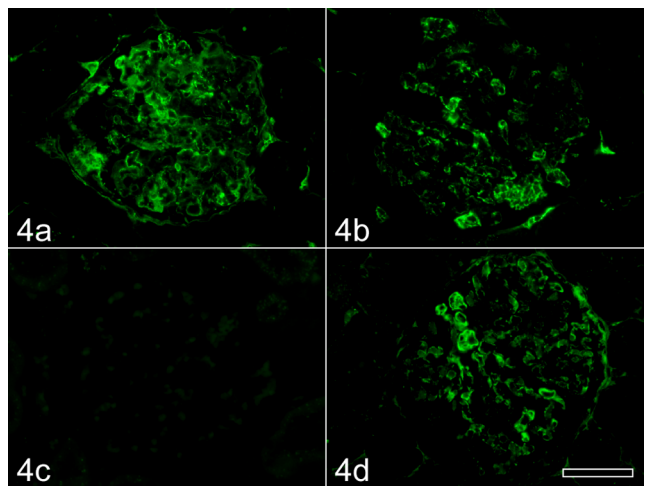


**Fig. 4.** Immunofluorescence of (a) anti-rat IgG, (b) anti-rat IgM, (c) anti-rat IgA, and (d) anti-rat C3 antibodies of the glomeruli of the Hatano low-avoidance (LAA) rat. Granular deposits of IgG, IgM and C3 are present in the mesangium and on the capillary wall of glomeruli. Bar = 50  $\mu$ m.

and fairly mild infiltration of CD68-positive macrophages within the mesangial areas were also detected. Segmental spike formation or bubble signs were fairly infrequently detected in the glomeruli by PAM staining. Immunofluorescence revealed granular deposits of IgG, IgM, and C3 in the glomeruli (Fig. 4), which were coincident with the red materials stained with Masson's trichrome stain. Deposition of IgG was most intense among the three Ig classes. Subepithelial dense deposits with irregular sizes and shapes were frequently observed by electron microscopy accompanied by occasional irregular thickening of the GBM (Fig. 5). The podocytes exhibited diffuse foot process effacement, reduc-

tion of slit diaphragms, rearrangement of the actin cytoskeleton in the fused foot process, formation of surface microvilli, and aberrant formation of cell-cell junctions between the neighboring foot processes. In addition, wedge-shaped interstitial mononuclear cell infiltration was observed in the left kidney. The renal tubules were occasionally cystic and contained proteinaceous casts, or were atrophic with a thick tubular basement membrane. Mild to moderate interstitial fibrosis was identified by Masson's trichrome staining (data not shown).

The results of Western blotting analysis are shown in Fig. 6. The sera from a normal SD rat and the present case



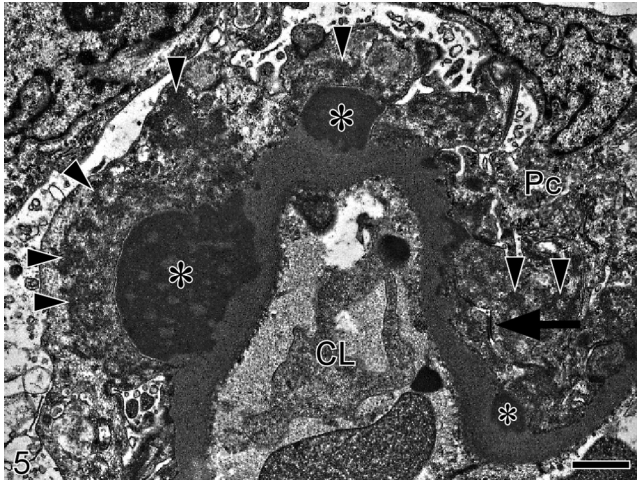


**Fig. 5.** Electron micrograph of the Hatano low-avoidance (LAA) rat glomeruli. Subepithelial dense deposits with irregular sizes and shapes are indicated by asterisks (\*). The podocytes exhibit diffuse foot process effacement, reduction of slit diaphragms, rearrangement of the actin cytoskeleton in the foot processes (arrowheads), and aberrant formation of cell-cell junctions between the neighboring foot processes (arrow). Transmission electron microscope. Pc, podocyte; CL, capillary lumen. Bar = 1  $\mu$ m.

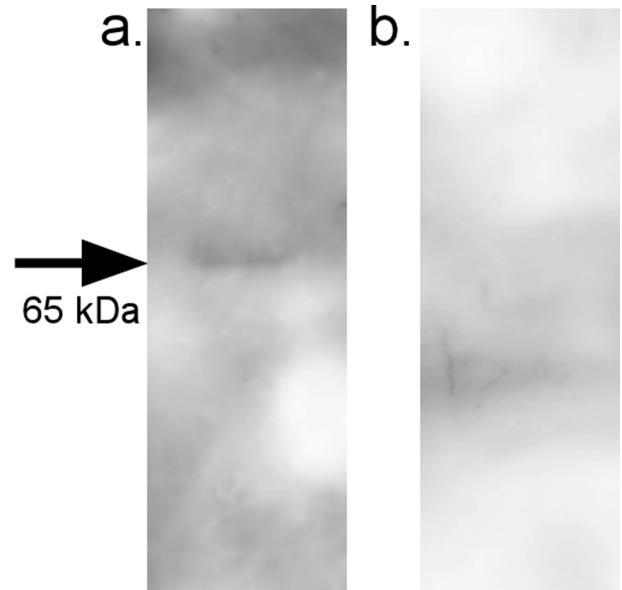


**Fig. 6.** Detection of autoantibody by Western blotting analysis. The protein from a fresh sample of Sprague-Dawley (SD) rat pancreas (1  $\mu$ g) is reacted with the serum from the present Hatano low-avoidance (LAA) rat (a) and a control SD rat (b). A single approximately 65-kDa band is detected using serum from the LAA rat (arrow).

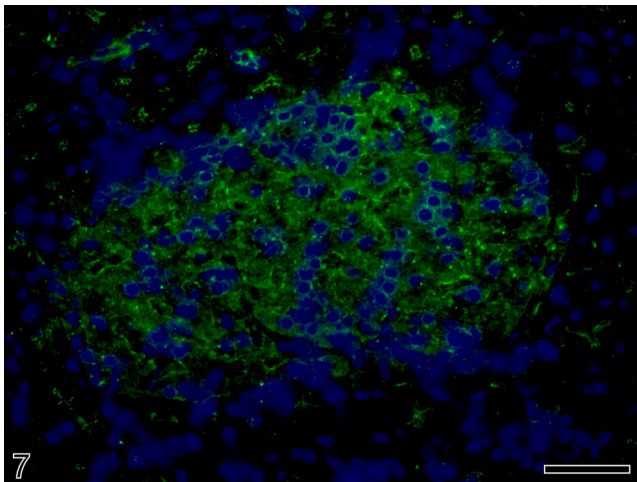


**Fig. 7.** Indirect immunofluorescence antibody test targeting normal rat (Sprague-Dawley rat) pancreas tissue using the serum from the present Hatano low-avoidance (LAA) rat. The cytoplasm of the islet cells shows weak reactions with the serum. Bar = 50  $\mu$ m.

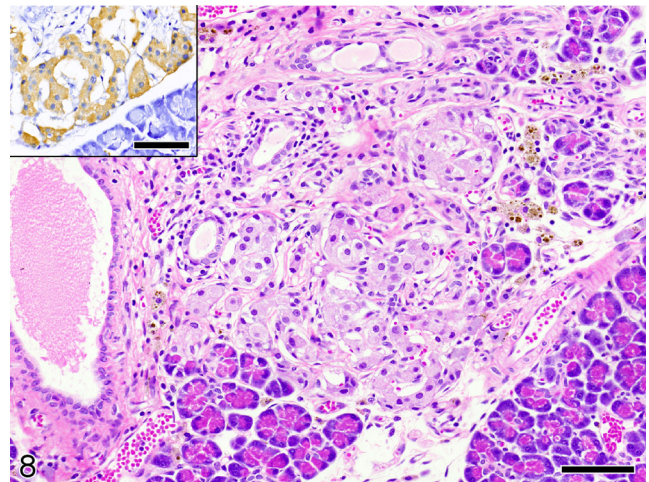


**Fig. 8.** Inflammation around the pancreatic duct with mild fibrosis and infiltration of lymphocytes and hemosiderin-phagocytic macrophages. Progressive proliferation of the islet cell population is observed within the lesion. Bar = 50  $\mu$ m. These proliferating islet cells usually contain insulin (inset). Immunostain. Bar = 50  $\mu$ m.

rat did not react with the liver samples, but the latter bound to the pancreas samples showing a single band of approximately 65–70 kDa. Indirect immunofluorescence revealed that the serum of the present case rat did not react with nuclei of either organ, but weakly reacted with the cytoplasm of the islet cells of the pancreas (Fig. 7).

Chronic inflammation was also observed in the pancreas (Fig. 8). Infiltration of CD3-positive and CD20-nega-

tive T lymphocytes was often observed diffusely within the pancreatic lobules, and these lesions were prominent around the pancreatic duct systems associated with the isolated proliferating foci of insulin-positive cells.

The mass on the right auricle was a fibrosarcoma with little inflammatory response. The tumor was partly ulcerated and attached firmly to the surrounding tissue, includ-

ing the auricular cartilage. Other organs were histologically normal, and no arthritis was observed at the articulation.

Chronic progressive nephropathy of the rats is an important differential diagnosis for this case. The SD rat commonly develops chronic progressive nephropathy with age, which is characterized by an increased mesangium and thickened basement membrane of the glomerular capillary loops and Bowman's capsules<sup>5,6</sup>. Nephropathy lacks the formation of dense deposits and is not immune-mediated. The histopathological characteristics of the glomerular lesions in the LAA rat were consistent with those of MN in humans and experimental animals. MN is classified into four stages according to the progression of the lesion<sup>7</sup>. The features of the glomerular lesions of the LAA rat, such as scattered immune deposits and rare formation of "spikes" in the GBM, might represent an early stage of MN. Therefore, the glomerulopathy observed in this case seems to be consistent with stage I MN. The focal interstitial mononuclear cell infiltration observed in the left kidney might not be related to glomerular lesions because the glomeruli were diffusely affected in both kidneys.

Idiopathic MN is usually considered to be an autoimmune disease, and exogenous antigens such as viral, bacterial, and tumoral antigens are thought to be involved in secondary MN following primary extrarenal diseases. In the past decade, tremendous progress has been made in understanding the molecular pathomechanism of human MN. Studies on clinical and experimental MN have led to the concept that podocyte antigens: megalin<sup>8</sup>, neutral endopeptidase (NEP)<sup>9</sup> or secretory phospholipase A<sub>2</sub> receptor (PLA<sub>2</sub>R1)<sup>10</sup> can be target antigens of idiopathic MN. However, mechanisms of immune complex deposition in the glomeruli in MNs are still controversial. Three hypotheses are proposed in recent studies: (1) the accumulation of circulating immune complexes and complements may result in the deposition of IgGs in the glomeruli, as was seen in chronic serum sickness<sup>11-13</sup>; (2) the immune complexes, including endogenous renal antigens as podocyte antigens<sup>8-10</sup>, can be formed *in situ* in the glomeruli; (3) or the immune complexes, including an exogenous antigen such as cationic bovine serum albumin<sup>14-16</sup>, can be formed *in situ* in the glomeruli. In this case, the LAA rat did not show evidence of infection or systemic autoimmune diseases associated with an antinuclear antibody, so these factors could be excluded from the pathogenesis of the present glomerulonephritis. Fibrosarcoma was observed in this rat, but the tumor might induce a poor immune reaction because of little inflammatory response to the tumor. In contrast, an antibody against the pancreas component was detected in serum of the present case by Western blotting and indirect immunofluorescence test. Pancreatic hormones such as insulin or glucagon were considered target antigens, but the molecular weight of the antigen detected by Western blotting was much bigger than these expected factors. However, an autoantibody against some pancreatic components might contribute to formation of circulating immune complexes or *in situ* immune com-

plex formation in the glomeruli.

Interestingly, several offspring from this rat showed the same pathologic lesions in the kidney and pancreas (data not shown). Within these cases, rats showing advanced chronic pancreatitis tended to develop glomerular injury. Chronic inflammation and parenchymal atrophy appear to be fairly common findings in the pancreas in aged rats<sup>17</sup>. They usually affect the pancreatic duct system, which suggests the ductal origin of this inflammation. During this process, the islet cells remain relatively unaffected but become disrupted in later stages of the disease<sup>18</sup>, as in the LAA rat. The relationship between chronic pancreatitis and development of an MN lesion is unclear; however, we should pay attention to glomerular lesions in cases with advanced chronic pancreatitis.

**Acknowledgments.** This research was partially supported by a research project grant awarded by the Azabu University. We are thankful to the National BioResource Project for the Rat in Japan (<http://www.anim.med.kyoto-u.ac.jp/NBR/>) for providing cryopreserved embryos of the LAA strain of rats. We also thank to Miss Asuka Sakakida, Miss Saori Kohno, Miss Saki Kohno and Miss Tomomi Horikawa for their assistance in collection of specimens.

## References

1. Couser WG. Basic and translational concepts of immune-mediated glomerular diseases. *J Am Soc Nephrol.* **23**: 381–399. 2012. [[Medline](#)] [[CrossRef](#)]
2. Glasscock RJ. The pathogenesis of idiopathic membranous nephropathy: a 50-year odyssey. *Am J Kidney Dis.* **56**: 157–167. 2010. [[Medline](#)] [[CrossRef](#)]
3. Heymann G, and Wahlig H. Properdin level and antibody production in the rabbit during immunization with *Mycobacterium tuberculosis* and *Salmonella typhosa*. *Z Immun Exp Ther.* **118**: 57–72. 1959. [[Medline](#)]
4. Ohta R, Matsumoto A, Hashimoto Y, Nagona T, and Mizutani M. Behavioral characteristics of rats selectively bred for high and low avoidance shuttlebox response. *Cong Anom.* **35**: 223–229. 1995.
5. Jones TC, Mour U, and Hunt RD. *Urinary System, Monographs on Pathology of Laboratory Animals.* Springer-Verlag, Berlin, Germany. 1986.
6. Simms HS, and Berg BN. Longevity and the onset of lesions in male rats. *J Gerontol.* **12**: 244–252. 1957. [[Medline](#)] [[CrossRef](#)]
7. Wasserstein AG. Membranous glomerulonephritis. *J Am Soc Nephrol.* **8**: 664–674. 1997. [[Medline](#)]
8. Oleinikov AV, Feliz BJ, and Makker SP. A small N-terminal 60-kD fragment of gp600 (megalyn), the major autoantigen of active Heymann nephritis, can induce a full-blown disease. *J Am Soc Nephrol.* **11**: 57–64. 2000. [[Medline](#)]
9. Debiec H, Guigonis V, Mougnot B, Decobert F, Haymann JP, Bensman A, Deschenes G, and Ronco PM. Antenatal membranous glomerulonephritis due to anti-neutral endopeptidase antibodies. *N Engl J Med.* **346**: 2053–2060. 2002. [[Medline](#)] [[CrossRef](#)]
10. Beck LH Jr, Bonegio RG, Lambeau G, Beck DM, Pow-

- ell DW, Cummins TD, Klein JB, and Salant DJ. M-type phospholipase A2 receptor as target antigen in idiopathic membranous nephropathy. *N Engl J Med.* **361**: 11–21. 2009. [[Medline](#)] [[CrossRef](#)]
11. Couser WG, and Salant DJ. In situ immune complex formation and glomerular injury. *Kidney Int.* **17**: 1–13. 1980. [[Medline](#)] [[CrossRef](#)]
  12. Dixon FJ, Feldman JD, and Vazquez JJ. Experimental glomerulonephritis. The pathogenesis of a laboratory model resembling the spectrum of human glomerulonephritis. *J Exp Med.* **113**: 899–920. 1961. [[Medline](#)] [[CrossRef](#)]
  13. Wilson CB, and Dixon FJ. Quantitation of acute and chronic serum sickness in the rabbit. *J Exp Med.* **134**: 7–18. 1971. [[Medline](#)]
  14. Adler SG, Wang H, Ward HJ, Cohen AH, and Border WA. Electrical charge. Its role in the pathogenesis and prevention of experimental membranous nephropathy in the rabbit. *J Clin Invest.* **71**: 487–499. 1983. [[Medline](#)] [[CrossRef](#)]
  15. Border WA, Ward HJ, Kamil ES, and Cohen AH. Induction of membranous nephropathy in rabbits by administration of an exogenous cationic antigen. *J Clin Invest.* **69**: 451–461. 1982. [[Medline](#)] [[CrossRef](#)]
  16. Debiec H, Lefeu F, Kemper MJ, Niaudet P, Deschenes G, Remuzzi G, Ulinski T, and Ronco P. Early-childhood membranous nephropathy due to cationic bovine serum albumin. *N Engl J Med.* **364**: 2101–2110. 2011. [[Medline](#)] [[CrossRef](#)]
  17. Greaves P. Liver and Pancreas In: *Histopathology of Pre-clinical Toxicity Studies*, 3rd ed. P Greaves (eds). Elsevier Science, Amsterdam, The Netherlands. 518-519. 2007.
  18. Spencer AJ, Andreu M, and Greaves P. Neoplasia and hyperplasia of pancreatic endocrine tissue in the rat: an immunocytochemical study. *Vet Pathol.* **23**: 11–15. 1986. [[Medline](#)]